

ARTICLE



New algorithm for corneal densitometry assessment based on anterior segment optical coherence tomography

Xiao Yu Wang^{1,4}✉, Tian Qiao Zhang², Anil Rahul Rachwani³, Irene Blanco-Domínguez¹, Carlos Rocha de Lossada¹, Alfredo Manuel Adán-Civiera¹ and Jorge Peraza-Nieves^{1,4}

© The Author(s), under exclusive licence to The Royal College of Ophthalmologists 2021

PURPOSE: To describe a new algorithm to measure corneal densitometry based on images obtained by swept source anterior segment ocular coherence tomography (SS-AS-OCT) and establish standard densitometry values in a group of normal eyes.

METHODS: A total of 111 healthy participants (195 eyes) were enrolled in this study. Using a MATLAB designed algorithm, the cornea was segmented into three layers: anterior, posterior and mid-stroma, and it was divided into two concentric areas, 0–2 and 2–4 mm, resulting in nine areas for the analysis. The mean corneal densitometry values were calculated and expressed as grayscale units (GSU).

RESULTS: The mean age was 57 years (range 22–87), with 100 (51.3%) right eyes and 95 (48.7%) left eyes. The total corneal densitometry was 86.9 ± 12.1 GSU. The mid-stroma layer had the highest densitometry values, 87.4 ± 12.1 GSU, and the anterior layer had the lowest values, 81.9 ± 14.2 GSU. Densitometry differences between the anterior layer and the mid-stroma layer ($P < 0.001$), as well as the anterior layer and the posterior layer ($P < 0.05$) were statistically significant. The 0–2 mm concentric area had higher mean densitometry values, 97.8 ± 12.7 GSU, and the differences were significant compared to the 2–4 mm concentric area ($P < 0.001$). No correlation was found between the corneal densitometry values and gender or age.

CONCLUSIONS: The new MATLAB segmentation algorithm for the analysis of corneal SS-AS-OCT images is capable to objectively assess corneal densitometry. We provide standard and normal data for better clinical and research approach.

Eye (2022) 36:1675–1680; <https://doi.org/10.1038/s41433-021-01707-7>

INTRODUCTION

Light can pass through a healthy cornea with little absorption and the light backscattering is minimal [1]. End stages of several corneal pathologies, such as corneal infections, dystrophies [2], degenerations, deposits [3] and ectasias [4, 5], may lead to corneal haze. Corneal densitometry has been introduced to objectively quantify corneal light backscatter (haze) via different devices. Kikkawa and Hirayama [6] used slit-lamp photography studies in an attempt to establish the relationship between corneal swelling and corneal light backscatter. Later on, the high-frequency ultrasound [7], confocal microscope through focusing [8, 9], Scheimpflug photography [10] and optical coherence tomography [11] had been used to study the corneal light backscatter. Studied areas vary from small specific points [12], individual layers [13] to partial surface areas [1]. Until recently, a comprehensive protocol using the Scheimpflug imaging system setup on Pentacam[®] (Oculus Optikgeräte GmbH, Wetzlar, Germany) with specific software to quantify the corneal densitometry values has been reported by Ni Dhubghaill et al. [14]. However, Scheimpflug devices generate lower quality images (blue light 475 nm, 1003×520 pixels [14]) compared to swept source anterior segment ocular coherence tomography (SS-AS-OCT) devices (laser 1050 nm,

1024×1200 pixels [15]) that obtain quasi-histological images (Fig. 1). With AS-OCT it is possible to measure the corneal thickness, epithelium thickness [16], precorneal tear film thickness, and tear meniscus height or area and even a corneal light backscattering have also been reported [11]. However, the corneal analysis is very limited compared to retina or glaucoma, and there is no report so far to the author's knowledge that attempted to quantify the corneal density by using AS-OCT.

The aim of this study is to design a novel algorithm based on high-quality SS-AS-OCT images, allowing us to quantify corneal density among healthy corneas and to describe its normal values.

METHODS

Participants

In this study, 195 eyes out of 111 consecutive subjects were evaluated by a cornea specialist from the Institut Clínic de Oftalmologia, Hospital Clínic de Barcelona. We excluded patients suffering from any ocular or systemic pathology or previous ocular surgery. All subjects signed an informed consent and agreed to the usage of their data for research purposes. This research was approved by the Hospital Clinic of Barcelona Research Ethics Board. The datasets consist of 195 images which are 6 mm radial pupil centred SS-AS-OCT scans and demographic

¹Institute of Clinic Ophthalmology, Clinic Hospital of Barcelona, University of Barcelona, Barcelona, Spain. ²School of Life and Environmental Sciences, Guilin University of Electronic Technology, Guilin, China. ³Ophthalmology Department, Hospital Regional de Málaga, Málaga, Spain. ⁴These authors contributed equally: Xiao Yu Wang, Jorge Peraza-Nieves. ✉email: xwanwan7@alumnes.ub.edu

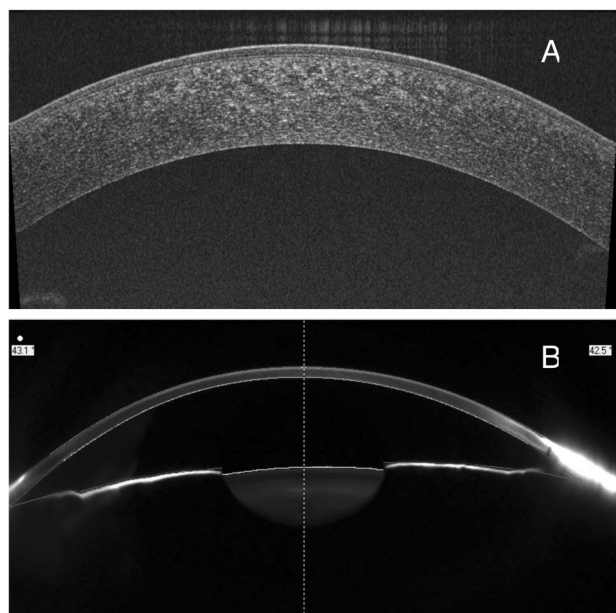


Fig. 1 The same corneal image by different image devices. **A** OCT and **B** Pentacam.

values. The entire study was conducted according to the tenets of the Declaration of Helsinki.

Swept source anterior segment optical coherence tomography

All corneal images were captured using the anterior segment module from the swept source OCT (SS-OCT) image device (DRI OCT Triton Plus, TOPCON, Tokyo, Japan). This device uses a 1050 nm wavelength light source performing 100,000 A-scans per second with an 8 μm in-depth resolution and 20 μm of lateral resolution. The size of each B-scan image captured was 1024 \times 1200 pixels. We selected the “anterior-Radial Anterior seg 6 mm” image function. Subjects were asked to look at the external fixation target. Later, images were manually clicked for caption with a joystick when the corneal top fixation position were achieved. All scans were taken by the same clinician using the same SS-OCT machine at same light environmental conditions.

Image segmentation protocol

Corneal scans were segmented and analysed by the described algorithm [17] using the MATLAB platform (version R2091a, MathWorks, Inc. Natick, MA, USA) (Fig. 2).

Three layers division. The algorithm firstly detected three anatomical boundaries:

- (1) Tear film–epithelium, due to the hyperreflective characteristic of this tear film, the boundary was programmed 3 pixels (15 μm) into the epithelium in parallel with it to avoid this artefact (upper green line).
- (2) Bowman’s membrane (blue line).
- (3) Endothelium (red line). The program built a parallel boundary to the endothelium line (red line) 50 μm into the stroma to create a fourth curved line (lower green line). The purpose to select 50 μm of tissue above the endothelium–aqueous boundary was to include the endothelial cells, the Descemet membrane (DM) and the DM–posterior stroma anatomical interface as a unit for the analysis. The DM thickness varies with age, habitually the anterior layer is approximately 3 μm and remains stable at all ages but the thickness of the posterior non-banded layer of DM increases with age, averaging \sim 2 μm at age 10 years and 10 μm at age 80 years [18]. A typical human endothelial cell measures 5 μm in height [19]. Taking care of these dimensions we hypothesised that 50 μm above the posterior boundary might be enough to assess this posterior layer.

Three main layers were created: epithelium, mid-stroma and posterior 50 μm of the cornea.

Three radial divisions. The algorithm set a tangent line to the corneal apex, and an auxiliary perpendicular line to this interception (black line) was drawn and displaced laterally 1 and 2 mm to each side. Four interception points were obtained at the tear film–epithelium layer and four correspondent tangent lines were drawn. Then, four segmentation lines (red lines) perpendicular to the four tangent lines were set.

Nine corneal segments. With three layers and four segmentation lines, we obtained nine corneal areas for the analysis:

- (1) Three central areas (2 mm): anterior (including the Bowman’s membrane), mid-stroma and posterior.
- (2) 2 \times 3 paracentral areas, one each side (2–4 mm): anterior, mid-stroma and posterior.

The algorithm obtained mean values of the densitometry of nine corresponding areas by using this formula: adding up all the densitometry values in each pixel of the corresponding area and dividing by the total number of pixels. The data were exported to the Excel sheet automatically. The results were expressed as grayscale units (GSU) range from 0 to 255, 0 meaning minimum light backscattering (maximum transparency) and 255 defines the maximum light density (minimum transparency). The MATLAB software was run in a personal computer with 64-bit Windows, Intel (R) Core (TM) i5-4460S CPU at 2.90 GHz and 8 GB RAM.

Statistical analyses

All results data were collected in Excel 2019 for Macintosh (version 16.32, Microsoft, Redmond, WA). Statistical analyses were carried out using SPSS Version 25 (IBM, Armonk, NY) and GraphPad Prism 8 (GraphPad, Inc., La Jolla, CA) for Macintosh. All datasets were tested for normality distribution using the D’Agostino and Pearson test and Kolmogorov–Smirnov test. Intraclass correlation coefficient (ICC) was calculated based on two repeated measurements of ten eyes (of ten different patients) by two operators to assess the reliability of the measurements using SPSS. One-way analysis of variance (ANOVA) test was used to analyse the differences between the corneal densitometry values within different layers and concentric areas. Pearson’s correlation tests were performed to examine the correlations between the two eyes of the same participants and densitometry relationship with ages. The independent samples *t*-test was used for the differences between the male and female groups. The results are represented as mean \pm standard deviation. All $P < 0.05$ were considered statistically significant within a 95% confidence interval.

RESULTS

Demographic features

In this study, 111 healthy participants were included, with a dataset of 195 eyes (including 95 right eyes 48.7.1% and 100 left eyes 51.3%). The mean age was 57 years (range 22–87). All participants were Caucasian and the demographic features are presented in Table 1. Based on our study, the standard deviation of total corneal densitometry was 12 (GSU), with a 95% confidence interval and a sample size of 195 eyes, resulting in a 0.4 margin of error, hence indicating a good sample size.

Corneal densitometry

The ICC results are shown in Table 2. The average ICC was 0.972 \pm 0.011, meaning excellent reliability. The mean values and the standard deviation of corneal densitometry of the overall measured areas were 86.9 \pm 12.1 GSU. All mean values of the 12 areas are summarised in the Table 3. The right and the left eye of the same subject were moderately correlated based on Pearson’s correlation test results (with all Pearson correlation coefficient values (*r*) higher or equal than 0.48). When dividing the cornea by layers from anterior to posterior, the highest mean values were in the mid-stroma layers (87.4 \pm 12.1 GSU). The lowest mean value was found in the anterior layer (81.9 \pm 14.2 GSU). There were significant differences between the anterior layer and mid-stroma layer (one-way ANOVA, $P < 0.001$) and between the anterior and the posterior layers ($P < 0.05$) (Fig. 3). In terms of different annuli, the 0–2 mm central area had a higher mean value of 97.8 \pm 12.7

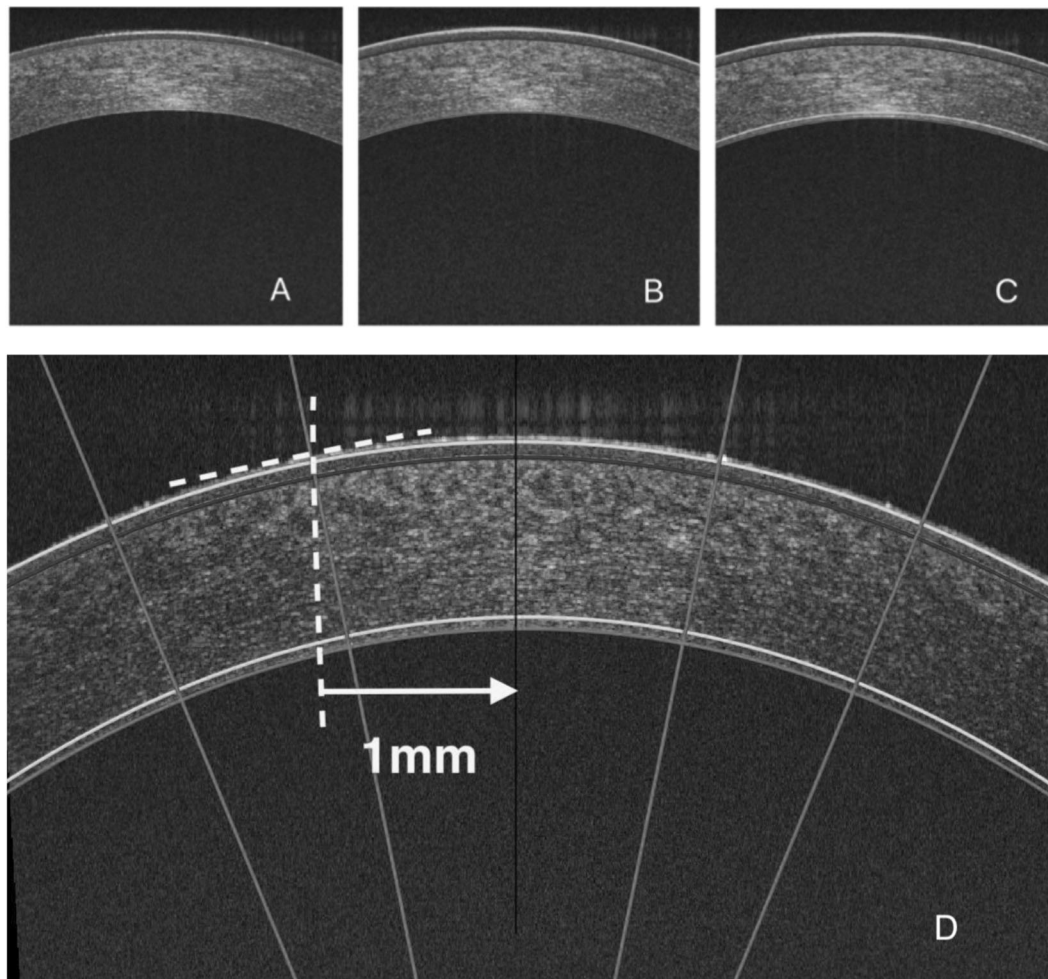


Fig. 2 The corneal image segmentation process. **A** Original AS-OCT image. **B** With two layers segmented: epithelium (between green line and blue line) and rest of cornea (between blue line and red line). **C** With three layers segmented: epithelium, post 50 μm of cornea (between lower green line and red line) and mid-stroma (between blue line and lower green line). **D** With three layers and three concentric areas segmented. *Black line corresponds the apical of the cornea. The dotted yellow line in parallel of the black line defines one intersection point with epithelium (the upper green line). The second dotted yellow line represents the tangent line of this intersection point.

Table 1. Demographic feature.

Category	Frequency (n)	Percentage (%)
Mean age (years)	57.16 (SD = 19.96)	Range 22–87
Gender	N = 111	100%
Male	50	45.0
Female	61	55.0
Eye	N = 195	100%
OS	100	51.3
OD	95	48.7

GSU than the 2–4 mm concentric area 76.4 ± 12.2 GSU and the differences were statistically significant ($P < 0.0001$).

Corneal densitometry in relation to gender and age

In this study, female patients had a higher mean corneal densitometry value of the total measuring areas (87.5 ± 12.3 GSU) compared to male patients (85.4 ± 12.5 GSU). However, differences in mean corneal density values between both genders were not statistically significant ($P = 0.37$, independent *t*-test).

The total corneal densitometry mean values were not significantly correlated between different ages (Pearson $r = 0.135$, $P = 0.058$),

Table 2. Intraclass correlation coefficient (ICC) based on two repeated measurements of ten eyes by two operators.













	Anterior	Central	Posterior	Total
0–2 mm				
ICC	0.980	0.972	0.986	0.971
2–4 mm				
ICC	0.948	0.971	0.955	0.964
Total				
ICC	0.966	0.974	0.979	0.972

neither between different annulus areas [0–2 mm ($r = 0.093$, $P = 0.191$) and 2–4 mm annulus ($r = 0.168$, $P = 0.185$)]. Correlation was not statistically significant between all three layers with $r = 0.113$, $r = 0.139$ and $r = 0.115$ for anterior, mid-stromal and posterior layers, respectively.

DISCUSSION

In our study, we report an innovative and descriptive approach to objectively assesses corneal density for the first time reported in the literature. We achieved this by using a SS-OCT imaging system

Table 3. Corneal densitometry mean and standard deviation values in each layer and concentric area and Pearson correlation (r) between the two eyes.

	0–2 mm	2–4 mm	Total
Anterior			
	84.37 ± 14.00	79.15 ± 14.66	81.94 ± 14.24
r	0.619	0.617	0.627
Central			
	99.23 ± 12.94	76.15 ± 12.00	87.42 ± 12.09
r	0.487	0.632	0.563
Posterior			
	98.73 ± 12.78	74.43 ± 13.07	86.52 ± 12.27
r	0.565	0.643	0.661
Total			
	97.77 ± 12.70	76.40 ± 12.19	86.86 ± 12.12
r	0.511	0.636	0.581

All values are in grayscale units (GSU).

in a large group of healthy eyes establishing the standard corneal densitometry value of 4 mm pupil-centred corneal area.

We found that the mid-stroma has the greatest densitometry values compared to the anterior and posterior layers, and the anterior layers had the lowest densitometry values. There are four major determining factors that explain the non-homogenous corneal light backscattering in a normal cornea: the refractive indices, the hydration gradient state across the cornea, keratocyte distribution density and the structural organisation of corneal lamellae. The refractive index of the epithelium was found to be greater than any other layers of the cornea and it varies along with the corneal depth [20]. Komai and Ushiki [21] demonstrated hydration gradients across the bovine cornea and found that corneal water content increases with corneal depth. This hydration gradient may also contribute to the light-backscattering gradient across the cornea. The region with greatest hydration (most posterior) induces the highest light backscattering and the layer with least hydration producing the least. Keratocytes nuclei are also a part of the OCT-detected backscatter causes, specifically by specular reflection. Studies indicate that the keratocyte distribution density in the human cornea is greatest in the anterior stroma [22–24]. The central stroma is rich in large collagen fibres lacking nucleus and other organelles that produce light backscattering. The structural characteristics of each corneal layer could also play a role. The organisation of the corneal lamellar structure shows a narrowed weaving pattern in the anterior stroma, whereas in the posterior stroma, the organisation is converted into a plane pattern [25]. Thus, the gradient of the mean corneal densitometry values could be due to differences in refractive indices across the cornea, differences in hydration in the axial direction, differences in lamellar structure and differences in the ratio of keratocytes. Thus, corneal density might be the result of combination of all these factors. Smith et al. [26] concluded that light backscattering

is higher in the anterior and posterior surface of the cornea than in the mid-stroma. Similarly, Rozema et al. [27] also found two distinguished peaks in the backscattering profiles: a strong epithelium–Bowman peak and a dimmer Descemet–endothelial peak. All these studies are consistent with our results: central stroma has higher corneal densitometry values than the anterior and posterior layers. However, partial consensus has been reached with studies by Garzón et al. [28] and Ni Dhubghaill et al. [14], which also found higher values in the anterior layer but lowest in the posterior layer. The controversy of this different finding could be the results of including the hyperreflective interface of the tear film–epithelium into the analysis.

When we look at different annuli, our work has yielded the same results as seen in previous studies: the central 0- to 2-mm annulus has higher corneal densitometry than the paracentral 2- to 4-mm annulus [14, 28]. There is a tendency to increasing the density readings from the central to the limbus, but not simple as linear pattern based on the Scheimpflug devices results: highest in the 10- to 12-mm annulus, then in the 6- to 10-mm annulus, 0- to 2-mm annulus and 2- to 6-mm annulus [14, 28]. This pattern of density reading gradient difference was not clear yet, but the high values of the limbus areas are mainly because of the senile annulus and histological transitional region from corneal to sclera. Due to the limitation of our work, we do not include all range but the first two annulus of cornea for the analysis, it would be interesting to conduct further study to include the whole cornea and limbal area to confirm this.

Controversial reports in corneal densitometry values related to patients' gender have been described. Garzón et al. [28], Ni Dhubghaill et al. [14] and Olsen [29] reported no relationship between corneal densitometry and gender using Pentacam, consistent with our results. However, Hillenaar et al. [12] found 3.5% higher light backscattering in men by using confocal

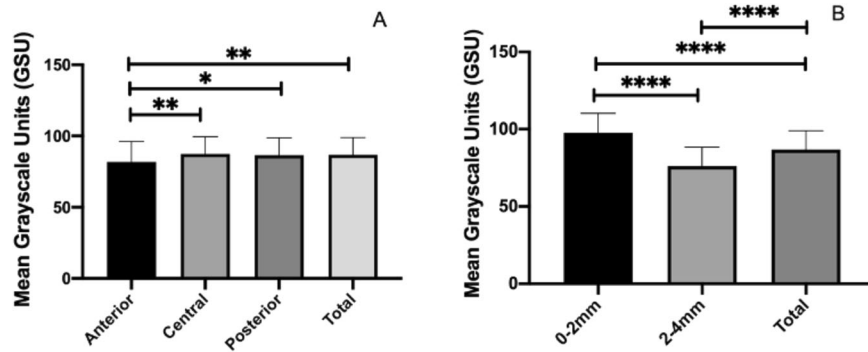


Fig. 3 Corneal Densitometry values based on different layers and concentric areas. **A** layers and **B** concentric areas, *($P < 0.05$), **($P < 0.001$), ****($P < 0.0001$).

microscopy. This might be explained due to differences between imaging system and analysis protocol used by these works. More studies are required to explain the relationship between densitometry and gender.

Previous studies [14, 19, 27] have reported that the total corneal densitometry values were positively correlated with age; specifically, old corneas tend to be clinically less transparent than young ones. But it also depends on the senile peripheral annulus, as densitometry increases while approaching to the limbus area (10–12 mm) and tends to decrease in the central 0–6 mm of the corneas analysed with Scheimpflug devices [14]. However, in our study, the studied areas were the 0–4 mm annulus of the corneal. Therefore, the influence by aging was minor, which is consistent with the results of the central annulus (0–2 mm) of the reported studies.

Our work provides a novel method to objectively assess corneal densitometry in a non-contact fashion by using high-quality images of SS-OCT imaging system unlike Scheimpflug images. The SS-OCT device has a different light source and longer wavelength (1050 nm), implying better tissue penetration, especially in the corneal tissue, compared to the Pentacam® device, which results in a superior image quality. Nevertheless, SS-OCT devices account for certain limitations. For instances, all images in this study were obtained using a manual shooting model, unlike Pentacam®, that incorporates an auto-focus and auto-release software. Otherwise, we only assessed the densitometry of one cross-section (horizontal meridian 0° – 180°) of the whole cornea and 0–4 mm pupil-centred corneal areas of this cross-section. Therefore, further studies are required to take into consideration the whole cornea and extend the scanned range. Our densitometry readings are higher than those observed in Pentacam system, our grey scale (0–255 GSU) differs from Pentacam scale (0–100 GSU); these higher values could be attributed to different image processing approach that could not be interchangeable as the different light sources (LED versus laser) of two different devices, different image analysis protocol and different reading scale, which cannot be directly (quantitatively) compared and results are not transferable between the different devices. Moreover, it would be interesting to expand this study by including more participants and describe the behaviour of corneal densitometry in some corneal pathologies. The clinical relevant of this finding is that we can compare the evolution of this parameter and correlate with pathologic events causing corneal leukoma, haze and interphase syndrome after LASIK, corneal dystrophies or stromal oedema due to endothelial damage; thus, it could be useful in the prediction of some pathologies improving the diagnosis processes and help the physician to decide the adequate moment for a medical and/or surgical intervention such as deep anterior lamellar or penetrating keratoplasty, bettering the daily care of patient and objective follow-up.

CONCLUSIONS

In this study, we describe the design of a novel automatic method for assessing the corneal densitometry using SS-OCT imaging system. To the best of our knowledge, this method has not been reported before in the literature. More importantly, we provide standard values of corneal densitometry in healthy eyes.

Summary

What was known before

- Corneal optical density as a potential indicator for corneal healthy was underinvestigated.
- Scheimpflug devices based corneal densitometry protocol was the only objective way of quantifying the corneal optical density.

What this study adds

- The first time in attempt to measure the corneal density based on AS-SS-OCT devices.
- A new algorithm developed in MATLAB which is capable for the corneal image segmentation and then objectively assessing the corneal optical density.
- The corneal density based on this high-quality imaging device was set and the higher density readings were found in the mid-stroma layer and 0–2 mm annulus of the healthy cornea.
- The clinical relevance of this finding is that we can compare the evolution of this parameter and correlate with pathologic events causing corneal leukoma, haze and interphase syndrome after LASIK, corneal dystrophies or stromal oedema due to endothelial damage, and help the physician to decide the adequate moment for a medical and/or surgical intervention such as deep anterior lamellar or penetrating keratoplasty.

REFERENCES

1. Otri AM, Fares U, Al-Aqaba MA, Dua HS. Corneal densitometry as an indicator of corneal health. *Ophthalmology*. 2012;119:501–8.
2. Ha BJ, Kim TI, Choi SI, Stulting RD, Lee DH, Cho HS, et al. Mitomycin C does not inhibit exacerbation of granular Corneal dystrophy type ii induced by refractive surface ablation. *Cornea*. 2010;29:490–6.
3. Elflein HM, Hofherr T, Berisha-Ramadani F, Weyer V, Lampe C, Beck M, et al. Measuring corneal clouding in patients suffering from Mucopolysaccharidosis with the Pentacam densitometry programme. *Br J Ophthalmol*. 2013;97:829–33.
4. Greenstein SA, Fry KL, Bhatt J, Hersh PS. Natural history of Corneal haze after collagen crosslinking for keratoconus and corneal ectasia: Scheimpflug and biomicroscopic analysis. *J Cataract Refract Surg*. 2010;36:2105–14.
5. Gutierrez R, Lopez I, Villa-Collar C, Gonzalez-Mejome JM. Corneal transparency after cross-linking for keratoconus: 1-year follow-up. *J Refract Surg*. 2012;28:781–6.

6. Kikkawa Y, Hirayama K. Uneven swelling of the corneal stroma. *Investig Ophthalmol*. 1970;9:735–41.
7. Allemann N, Chamon W, Silverman RH, Azar DT, Reinstein DZ, Stark WJ, et al. High-frequency ultrasound quantitative analyses of corneal scarring following excimer laser keratectomy. *Arch Ophthalmol*. 1993;111:968–73.
8. Møller-Pedersen T, Cavanagh HD, Petroll WM, Jester JV. Corneal haze development after PRK is regulated by volume of stromal tissue removal. *Cornea*. 1998;17:627–39. <https://doi.org/10.1097/00003226-199811000-00011>.
9. Møller-Pedersen T, Vogel M, Li HF, Petroll WM, Cavanagh HD, Jester JV. Quantification of stromal thinning, epithelial thickness, and corneal haze after photorefractive keratectomy using in vivo confocal microscopy. *Ophthalmology*. 1997;104:360–8. [https://doi.org/10.1016/s0161-6420\(97\)30307-8](https://doi.org/10.1016/s0161-6420(97)30307-8).
10. Binder PS, Bosem M, Weinreb RN. Scheimpflug anterior segment photography assessment of wound healing after myopic excimer laser photorefractive keratectomy. *J Cataract Refract Surg*. 1996;22:205–12.
11. Wang J, Simpson TL, Fonn D. Objective measurements of corneal light-backscatter during corneal swelling, by optical coherence tomography. *Investig Ophthalmol Vis Sci*. 2004;45:3493–8.
12. Hillenaar T, Cals RH, Eilers PH, Wubbels RJ, van Cleynenbreugel H, Remeijer L. Normative database for corneal backscatter analysis by in vivo confocal microscopy. *Investig Ophthalmol Vis Sci*. 2011;52:7274–81.
13. Patel S, Winter EJ, McLaren JW, Bourne WM. Objective measurement of back-scattered light from the anterior and posterior cornea in vivo. *Investig Ophthalmol Vis Sci*. 2007;48:166–72.
14. Ní Dhubhghaill S, Rozema JJ, Jongenelen S, Ruiz Hidalgo I, Zakaria N, Tassignon MJ. Normative values for corneal densitometry analysis by Scheimpflug optical assessment. *Investig Ophthalmol Vis Sci*. 2014;55:162–8. <https://doi.org/10.1167/iovs.13-13236>.
15. Potsaid B, Baumann B, Huang D, et al. Ultrahigh speed 1050nm swept source/ Fourier domain OCT retinal and anterior segment imaging at 100,000 to 400,000 axial scans per second. *Opt Express*. 2010;18:20029–48. <https://doi.org/10.1364/OE.18.020029>.
16. Wang J, Fonn D, Simpson TL, Sorbara L, Kort R, Jones L. Topographical thickness of the epithelium and total cornea after overnight wear of reverse-geometry rigid contact lenses for myopia reduction. *Investig Ophthalmol Vis Sci*. 2003;44:4742–6.
17. Zhang T, Elazab A, Wang X, Jia F, Wu J, Li G, et al. A novel technique for robust and fast segmentation of corneal layer interfaces based on spectral-domain optical coherence tomography imaging. *IEEE Access*. 2017;5:10352–63.
18. Johnson DH, Bourne WM, Campbell RJ. The ultrastructure of Descemet's membrane. I. Changes with age in normal corneas. *Arch Ophthalmol*. 1982;100:1942–7. <https://doi.org/10.1001/archophth.1982.01030040922011>.
19. Tekin K, Sekeroglu MA, Kiziltoprak H, Yilmazbas P. Corneal densitometry in healthy corneas and its correlation with endothelial morphometry. *Cornea*. 2017;36:1336–42. <https://doi.org/10.1097/ICO.0000000000001363>.
20. Vasudevan B, Simpson TL, Sivak JG. Regional variation in the refractive-index of the bovine and human cornea. *Optom Vis Sci*. 2008;85:977–81. <https://doi.org/10.1097/OPX.0b013e3181886fa5>.
21. Komai Y, Ushiki T. The three-dimensional organization of collagen fibrils in the human cornea and sclera. *Investig Ophthalmol Vis Sci*. 1991;32:2244–58.
22. Patel S, McLaren J, Hodge D, Bourne W. Normal human keratocyte density and corneal thickness measurement by using confocal microscopy in vivo. *Investig Ophthalmol Vis Sci*. 2001;42:333–9.
23. Hahnel C, Somodi S, Weiss DG, Guthoff RF. The keratocyte network of human cornea: a three-dimensional study using confocal laser scanning fluorescence microscopy. *Cornea*. 2000;19:185–93.
24. Prydal JI, Franc F, Dilly PN, Kerr Muir MG, Corbett MC, Marshall J. Keratocyte density and size in conscious humans by digital image analysis of confocal images. *Am J Optom Physiol Opt*. 1998;12:337–42.
25. Ruberti JW, Roy AS, Roberts CJ. Corneal biomechanics and biomaterials. *Ann Rev Biomed Eng*. 2011;13:269–95.
26. Smith GT, Brown NA, Shun-Shin GA. Light scatter from the central human cornea. *Eye*. 1990;4:584–8. <https://doi.org/10.1038/eye.1990.81>.
27. Rozema JJ, Trau R, Verbruggen KH, Tassignon MJ. Backscattered light from the cornea before and after laser-assisted subepithelial keratectomy for myopia. *J Cataract Refract Surg*. 2011;37:1648–54. <https://doi.org/10.1016/j.jcrs.2011.03.043>.
28. Garzón N, Poyales F, Illarramendi I, Mendicutie J, Jáñez Ó, Caro P, et al. Corneal densitometry and its correlation with age, pachymetry, corneal curvature, and refraction. *Int Ophthalmol*. 2017;37:1263–8. <https://doi.org/10.1007/s10792-016-0397-y>.
29. Olsen T. Light scattering from the human cornea. *Investig Ophthalmol Vis Sci*. 1982;23:81–6.

ACKNOWLEDGEMENTS

The authors assume full responsibility for the analyses and interpretation of these data.

AUTHOR CONTRIBUTIONS

XYW and JP-N were responsible for conceiving the presented idea. XYW, JP-N, IBD and CRdL carried out the experiments. XYW and TQZ performed the computations. XYW and JP-N wrote the manuscript with the support from JP-N, IB-D, CR-d-L and ARR. Author AMA-C supervised the project. All authors provided critical feedback and helped shape the research, analysis and manuscript.

COMPETING INTERESTS

The authors declare no competing interests.

ADDITIONAL INFORMATION

Correspondence and requests for materials should be addressed to X.Y.W.

Reprints and permission information is available at <http://www.nature.com/reprints>

Publisher's note Springer Nature remains neutral with regard to jurisdictional claims in published maps and institutional affiliations.